# JOSEPHSON-LIKE PROPERTIES OF $YBa_2Cu_3O_7$ THIN FILM WEAK LINKS

D. K. Lathrop, S. E. Russek*, B. H. Moeckly, D. Chamberlain,
L. Pesenson, R. A. Buhrman, D. H. Shin and J. Silcox
School of Applied and Engineering Physics, Cornell University
Ithaca, NY 14853.2501

*Present address National Institute of Standards and Technology
Boulder, CO 80303

## Abstract

Thin film $YBa_2Cu_3O_7$ microbridges have been fabricated by photo- and e-beam lithography in poly-crystalline thin films grown on MgO substrates and containing a controlled density of large angle tilt boundaries, thereby isolating individual tilt-boundary weak links. Depending on the growth parameters of the film such weak links have critical current densities $J_C$ ranging from $< 10^4$ A/cm$^2$ to $> 10^6$ A/cm$^2$. The higher $J_C$ microbridges exhibit behavior indicative of one-dimensional flux flow and flux creep in the weak links while the lower $J_C$ microbridges have RSJ-like properties. Detailed comparisons have been made between the predictions of the RSJ model, including the calculated effects of thermal noise rounding, and the measured dc and microwave response of these weak links. Measurements have also been made of magnetic field effects on the critical current density. An unexpected scaling behavior has been observed in the I-V characteristics of certain types of these microbridges containing 45° tilt boundaries that indicates that in those cases $I_CR_N^2$ is a constant for the tilt boundary weak link. The implications of these results for developing a successful description of the superconductive properties of $YBa_2Cu_3O_7$ grain boundary weak links which electron microscopy reveals to be clean, stoichiometric and abrupt is discussed.

## Introduction

It has been rather well established that the presence of high angle tilt grain boundaries in c-axis-normal oriented high temperature superconducting (HTS) thin films can result in the superconducting transport properties of the film being weakened at or in the vicinity of the boundary in comparison to those properties when measured in the bulk film or at low angle (< 5° ) tilt boundaries[1,2]. Many of the most promising applications of HTS thin films such as passive microwave elements and thin film interconnects are quite demanding with regard to the critical current density $J_C$ of the film. Consequently even a factor of 10 reduction in $J_C$ below the values ($\geq 5 \times 10^6$ A/cm$^2$ at 77 K) that can be obtained in high quality epitactic films due to the presence of a significant density of such high angle tilt boundaries can be quite detrimental to the performance of the film. On the other hand there is widespread interest in the formation of high performance HTS thin film weak links and tunnel junctions for use as Josephson elements in SQUID and radiation sensor applications and, perhaps eventually, in other Josephson applications. Currently the most successful approach to the formation of Josephson-like weak link elements appears to be through the formation and isolation of high angle tilt boundaries (HATB). Consequently, it is rather important that the properties of HATBs be well understood at a fundamental level, and if at all possible, the reduction of $J_C$ at such boundaries be minimized. At the same time the Josephson-like properties of such boundaries should be carefully examined, both to evaluate the potential of such HATB weak links for significant Josephson sensor applications and to gain insight that should prove useful in the successful development of a true Josephson junction fabrication technology in HTS thin films.

$YBa_2Cu_3O_7$ thin films grown by laser ablation under certain conditions on (001) MgO substrates can readily form HATBs as result of the $YBa_2Cu_3O_7$ grains assuming different special epitactic orientations relative to the MgO. The regions of alternative rotations are typically several micrometers or greater in extent and thus these HATBs can be readily isolated by conventional lithography and ion milling for detailed study of their normal and superconductive properties. Depending on the quality of the $YBa_2Cu_3O_7$ grains forming the tilt boundary, and perhaps on the specific tilt boundary angle, the critical current density at 4.2 K of the HATB can vary from $< 10^4$ A/cm$^2$ to $> 10^6$ A/cm$^2$. In the former case self shielding of the supercurrent is not a major concern in thin film microbridges of $\leq 2$ μm in width and thus a detailed study of the intrinsic Josephson-like properties of the HATB can be undertaken. In the latter case, self shielding is quite significant and thus these devices can be employed for a detailed study of one-dimensional flux flow and flux creep along HATBs. Here we will describe various results of these studies and, as well, discuss a remarkable scaling law that we have recently discovered for the critical current density of 45° tilt boundaries as a function of tilt boundary conductance, and describe how this scaling law appears to change as the tilt boundary angle is reduced.

## Physical Properties

The $YBa_2Cu_3O_7$ films used in this study were produced by laser ablation on MgO substrates using standard conditions[3]. The films are oriented with the c-axis perpendicular to the plane of the substrate, but by carefully controlling the preparation of the MgO substrate prior to the deposition and adjusting the deposition conditions, the rotation of the $YBa_2Cu_3O_7$ a and b axes with respect to the MgO principal axes can be controlled. When the MgO substrate is mechanically polished then annealed (typically 1100 C, 24 Hrs.) prior to deposition, the resulting $YBa_2Cu_3O_7$ films' a and b axes are aligned with the substrates principal axes, resulting in a film with no HATBs and high $J_C$ ($\geq 5 \times 10^6$ A/cm$^2$ at 77 K, $\geq 5 \times 10^7$ A/cm$^2$ at 4.2 K). Alternatively, when the substrate is just mechanically polished, x-ray pole figures indicate that about 80% of the grains have their a and b axes oriented parallel to the MgO principal axes, while the rest of the grains are rotated 45° to this. And when the substrate is chemically polished, the pole figures show a wide variety of film-substrate rotations, including 45°, 27°, and smaller angles. This results in the presence of a large number of HATBs. Transmission electron microscopy studies[4] on these films reveal that the size of an area that is rotated by 45° is typically greater than 1 μm$^2$, as shown in Fig. 1. Fig. 2 is a transmission electron micrograph of a 45° grain boundary showing an abrupt, clean transition region only 2 - 3 nm wide[5]. Thus by patterning narrow microbridges in these films by conventional lithographic techniques, a single one of these grain boundaries can be isolated and studied.

In the case of films on mechanically polished substrates the density of HATBs is sufficiently low that many microbridges do not have any weak links. By comparing $J_C$ for microbridges with and without weak links we find that the presence of a 45° HATB generally results in the reduction of $J_C$ by approximately a factor of ten over that of the bulk film. For films grown on chemically polished substrates the density of HATBs is such that all microbridges show weak link behavior. The variation of this

Manuscript received September 24, 1990.

Figure 1: Transmission electron micrograph plan view of a 45° grain boundary. The straight, parallel lines running within grains are twin boundaries and indicate the orientation of the grain. The black irregularly curved line (most evident running left to right in the lower part of the picture) is the boundary between regions rotated 45° with respect to each other.

behavior with different tilt boundary angle has not been determined as yet.

In general for all the weak links we find that $J_C$ for the HATB weak links tends to scale inversely, and more rapidly than linearly, with the local bulk resistivity of the $YBa_2Cu_3O_7$ film in the microbridge region. This resistivity can be readily measured since the overall microbridge resistance is generally much larger than the resistance of the tilt boundary, which is temperature independent below $T_C$. The bulk resistivity of films grown on chemically polished substrates tended to be higher and hence $J_C$ was lower than was the case for the 45° tilt boundaries on mechanically polished substrates.

## Current-Voltage Characteristics

Figure 3 shows typical examples of current-voltage characteristics obtained in different microbridges as $J_C$ decreases from ~$10^7$ A/cm$^2$ to ~$10^4$ A/cm$^2$ at 4.2 K. For the higher critical current densities, as in Fig. 3a, the I-V curve exhibits the rapidly increasing resistance with increasing voltage that results from the onset of flux creep. The I-V curves from microbridges patterned on films with no HATBs typically exhibit this strongly non-linear behavior as well as very high $J_C$'s. A similar result is obtained with microbridges containing HATBs that are fabricated in otherwise very high quality, very low resistivity, films such that at 4.2 K the HATB has $J_C \geq 10^6$ A/cm$^2$.

Microbridges on films with a large number of HATBs, however, in general exhibit I-V curves like those in Fig. 3b and 3c. When $J_C$ is low enough that the Josephson penetration

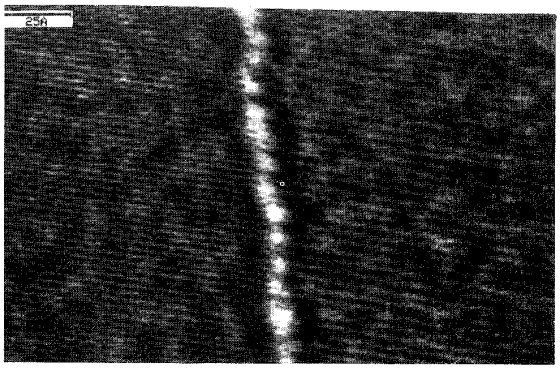

Figure 2: High resolution scanning transmission electron micrograph view of a 45° tilt grain boundary. The horizontal lines on the left are (110) lattice fringes, those on the right are (100) lattice fringes.

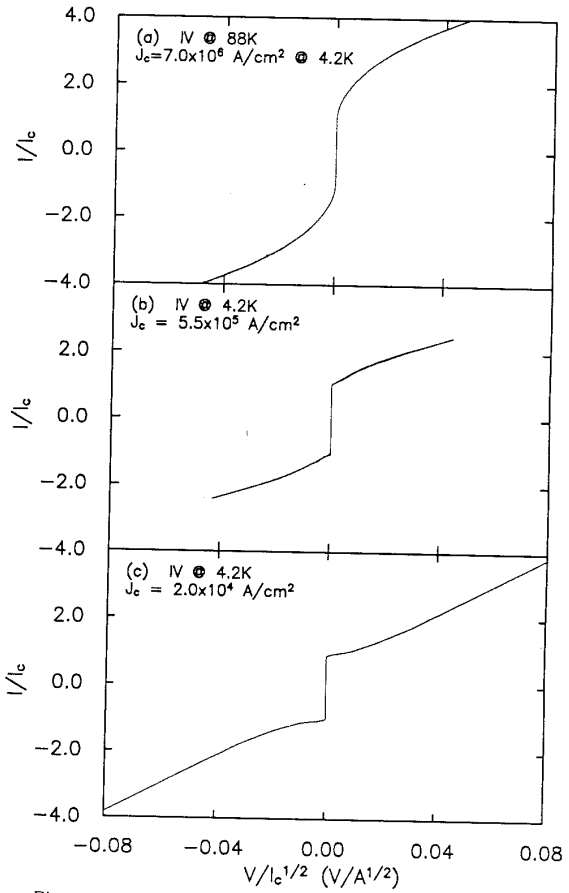


Figure 3: Typical I-V characteristics. a) High $J_C$ microbridge exhibiting flux creep behavior. b) Mid $J_C$ weak link showing linear voltage onset and flux flow. c) Low $J_C$ weak link exhibiting good RSJ behavior.

depth $\lambda_J$ is larger than the width of the microbridge, self shielding effects are absent and the I-V curve can be well modeled by the resistively shunted junction (RSJ) model, as in Fig. 3c. For somewhat higher $J_C$, $\lambda_J$, which is proportional to $J_C^{-1/2}$, becomes less than the width of the microbridge. At this point self shielding effects become apparent in the form of "excess current"[6] in the I-V characteristic, due to one-dimensional flux flow. Even higher $J_C$ results in a I-V curve like that in Fig. 3b, which exhibits a linear onset of voltage with increasing current, and can be attributed to flux flow.

For the lowest $J_C$ microbridges, which exhibit RSJ-like I-V characteristics, deviations from the RSJ model can sometimes be observed. Close inspection of the I-V curves taken at low temperature (4.2 K) reveal small resonances at constant voltages. Such deviations are similar to those seen in high quality low temperature superconductor microbridges[7] and is generally attributed to ac supercurrent resonance effects established by the electrode structure. This self-resonance effect is apparently due to a cavity established by the overall electrode structure, rather than an excessively high dielectric constant as suggested by Mannhart et. al.[8] in a study of $YBa_2Cu_3O_7$ grain boundaries formed by growth on $SrTiO_3$ bicrystals. As the temperature is increased, these resonances are washed out, as is the sharp onset of voltage predicted by the RSJ model. This is the effect of thermal noise and is very well modeled by the standard noise theory[9,10], as shown in Fig. 4.

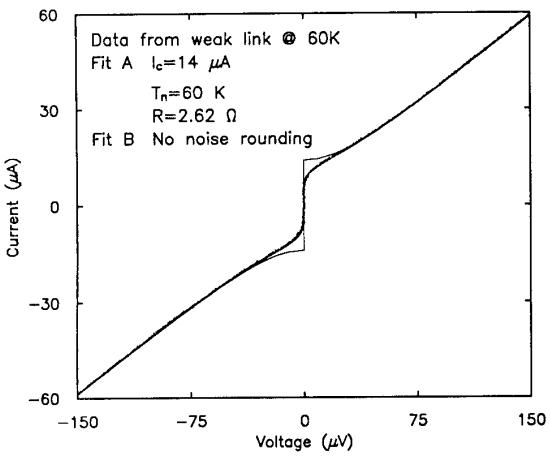


Figure 4: I-V curve at 60 K showing effects of thermal noise rounding. Fit A includes noise rounding and on this scale is indistinguishable from the data. Fit B does not include noise rounding and shows a sharp voltage onset.

## Magnetic Field Effects

In a small magnetic field, the critical current of a uniform rectangular weak link with minimal screening of the applied field will oscillate in a manner similar to a Fraunhofer diffraction pattern,

$$I_C = I_{C0} \frac{\sin(H/H_0)}{H/H_0} \qquad (1)$$

with the period $H_0$ given by

$$H_0 = \Phi_0 w(d+2\lambda_L). \qquad (2)$$

Here $\Phi_0$ is the flux quantum (h/2e), w is the width of the junction, d is the thickness of the normal (or insulating) region, and $\lambda_L$ is the London penetration depth. This should be valid as long as the width w is less than $\lambda_J$, as in our lowest $J_C$ devices. Assuming a low temperature value of $\lambda_L$ = 1500 Å, w = 1 μm, and $d<<\lambda_L$ we obtain an expected oscillation period of 6.2 Gauss for a typical $YBa_2Cu_3O_7$ weak link. A weak link whose $J_C$ is nonuniform will still exhibit a critical current whose magnitude oscillates with magnetic field, but the successive maxima will not follow a sin(x)/x behavior, and the minima may not reach zero[11].

In Figure 5, the behavior of a typical weak link in small magnetic field is presented and is useful for illustrating four points. First, the maxima do not follow a sin(x)/x behavior, and in fact the fourth maxima is 80% the height of the central peak. Since self shielding effects should not be effective for this low $J_C$ weak link this suggests that the grain boundary is nonuniform, consisting of a few areas (perhaps 3 to 5) of good superconducting contact with widths about 5 - 10 % the full width of the microbridge, as the possible simulation in Figure 5 shows. Second, the minima do not reach zero, which simply means that the weak link is asymmetric about its center. Third, the critical current experiences abrupt jumps, which we believe is the effect of flux jumping into or out of adjacent grains. In fact these jumps occur approximately every 20 - 40 Gauss, which is consistent with an area of 1 - 2 $\mu m^2$ for the grains. And finally, the periodicity is ~ 10 Gauss, which is consistent with the expected periodicity for this size microbridge (1.2 μm wide), indicating that $\lambda_L$ in the vicinity of the tilt boundary is fairly close to the expected bulk value.

In high $J_C$ microbridges, the critical current decreases monotonically with field up to at least 3 Tesla. Initially $I_C$ decreases smoothly by 25% to 75% to 0.5 Tesla. Above 0.5 Tesla, $I_C$ is proportional to $e^{-H/\beta}$, with β ~ 0.5 to 5 Tesla, consistent with the results recently reported by Hampshire et. al.[12]. These studies of the effects of high magnetic fields on high $J_C$ (>> $10^5$ A/cm² at 4.2 K) HATBs are continuing and will be reported in more detail elsewhere.

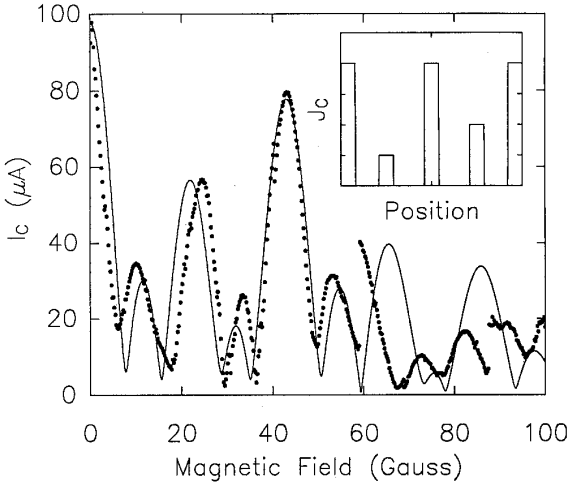


Figure 5: $I_C$ vs. H for a weak link where $\lambda_J$ is greater than the width of the microbridge. The line is a theoretical prediction assuming the $J_C$ vs. position shown in the inset.

## Critical Current vs. Temperature

Figure 6 presents the critical current as a function of temperature over the entire temperature range for a HATB with a $J_C$ ~ $10^5$ A/cm² at 4.2 K. This represents a microbridge where self-screening effects are beginning to be apparent, i. e. it exhibits excess current, but the major features of $I_C$ vs. T as shown in Fig. 6 are typical of all the microbridges discussed in this work.

Above 80-90% of $T_C$, $I_C$ can generally be fit reasonably well by the functional form

$$I_C \propto (1-T/T_C)^N \qquad (3)$$

where N ≥ 1.5. Figure 7 shows $I_C$ vs. T near $T_C$ and fits to $(1-T/T_C)^{3/2}$ for three microbridges covering the entire range of

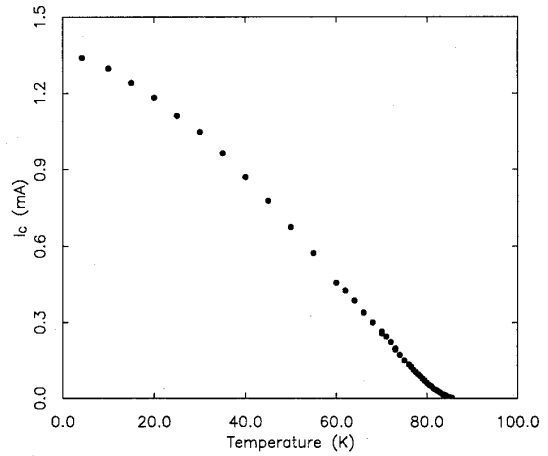


Figure 6: $I_C$ vs. T for a 45° tilt boundary weak link.

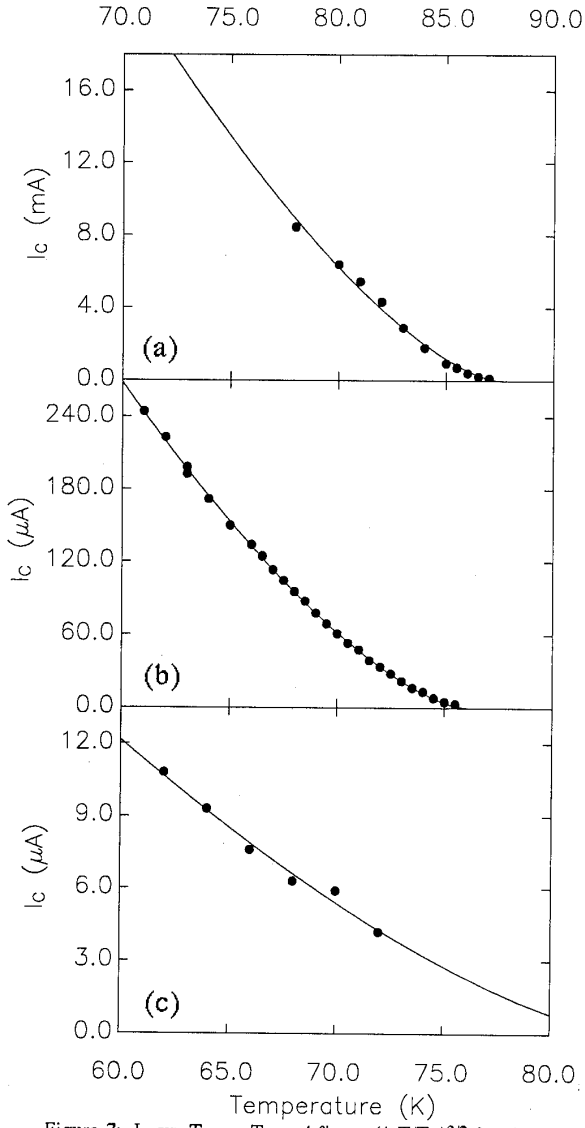


Figure 7: $I_C$ vs. T near $T_C$ and fits to $(1-T/T_C)^{3/2}$ for three microbridges spanning three orders of magnitude in $I_C$. a) High $J_C$ microbridge (> $10^7$ A/cm$^2$ at 4.2 K). b) 45° tilt boundary, $J_C$ ~ $3\times10^5$ A/cm$^2$ at 4.2 K. c) 45° tilt boundary, $J_C$ ~ $2\times10^4$ A/cm$^2$ at 4.2 K.

$J_C$ examined, from $10^4$ A/cm$^2$ to $10^7$ A/cm$^2$ at 4.2 K. If we fit to $(1-T/T_C)^N$, most of the weak links examined yield an N of 1.5 to 2, with the remainder giving an N greater than 2. Given the evidence from the magnetic field dependence of $I_C$ that these weak links are nonuniform, we might also assume that $T_C$ varies slightly across the width of the microbridge. Such variations in $T_C$ will have the effect of raising the apparent value of N measured in such a microbridge. Indeed, if we also look at the overall resistive transition of these microbridges, we find that the sharper the resistive transition, and the closer the extrapolated $T_C$ of the weak link is to the zero resistance point of the resistive transition, the closer N is to 1.5. We take this to strongly suggest that measurements of N ~ 2 simply represent a nonuniformity in $T_C$ along the tilt boundary, similar to the nonuniformity in $J_C$ evident from the magnetic field behavior, and does not indicate the presence of a narrow normal layer at the tilt boundary as would be suggested by N = 2. This latter hypothesis is of course also incompatible with the measured conductance of the weak link (G ~ $10^8$-$10^9$ S/cm$^2$) being much less than that of a normal conductor of ~3 nm in length.

## Microwave response

Figure 8 shows a typical I-V curve at 4.2 K with 10 GHz microwaves applied, displaying the expected constant voltage steps at integral multiples of V=hν/2e. Given the size of the resultant steps, thermal noise rounding is evident and has a significant effect on the apparent amplitude of the steps if measured directly. In order to take this into account and measure the step size as a function of microwave power, the amplitude of the steps was measured by fitting them to the RSJ model with noise rounding in the small capacitance limit. The fits were performed on the I-V curves in the vicinity of each step, with the step height, current offset, and voltage offset as parameters and the resistance fixed at the measured value in the absence of microwaves. Although the measurements were performed at 4.2 K, the effective noise temperature at which the best fit was obtained in the absence of microwaves was somewhat higher than this, 8-10 K, due to noise from outside the cryostat.

As the microwave power to the weak link is increased, and the critical current decreases, the apparent noise temperature which yields the best fit increases. This is illustrated in Figure 9, which shows I-V data at two microwave power levels along with fits at various noise temperatures. The apparent noise temperature for the N=0 step increases to 40-50 K at the first zero of the N=0 step; further increasing the microwave power, with the step size oscillating as expected, does not increase the apparent noise temperature any more. For the N=1, 2, and 3 steps, the noise temperature which yields the best fit when the steps are near their maximum is 35 to 50 K. When this effect is taken into account, by using a noise temperature of 40 K in the fits above the first zero of the N=0 step, the agreement of step amplitude vs. microwave power with theory is remarkably good through 3 or 4 oscillations of the N=0 step.

The elevation of the apparent noise temperature could be an artifact of the measurement and analysis, possibly due to the assumption in the analysis of a sinusoidal current-phase relation. This view is supported by the fact that when similar measurements are made at higher ambient temperatures, T ~ 40 K, a similar apparent increase in the noise temperature is found with increasing microwave power, but now starting from $T_N$ = 40 K. Numerical simulations without noise and with a distinctly nonsinusoidal current-phase relation generally show small subharmonic steps at positions close to the major steps. The presence of thermal noise in the real case will completely wash out these subharmonic steps, but their presence will cause the normal steps to appear more rounded.

For microbridge weak links which have $I_C$ sufficiently large that noise rounding is not excessive, periodic response to rf

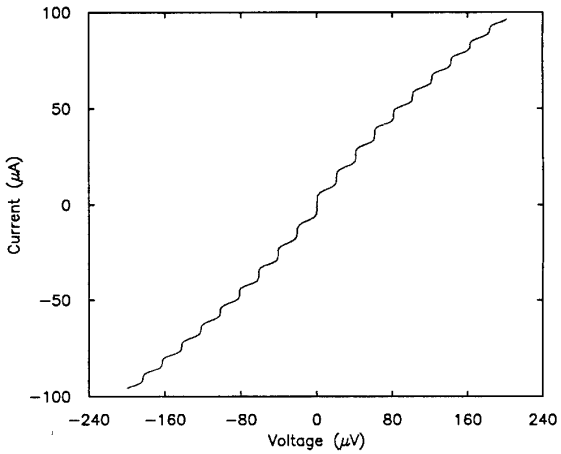


Figure 8: I-V curve with ~10 GHz microwave radiation exhibiting constant voltage at integral multiples of ~20 μV.

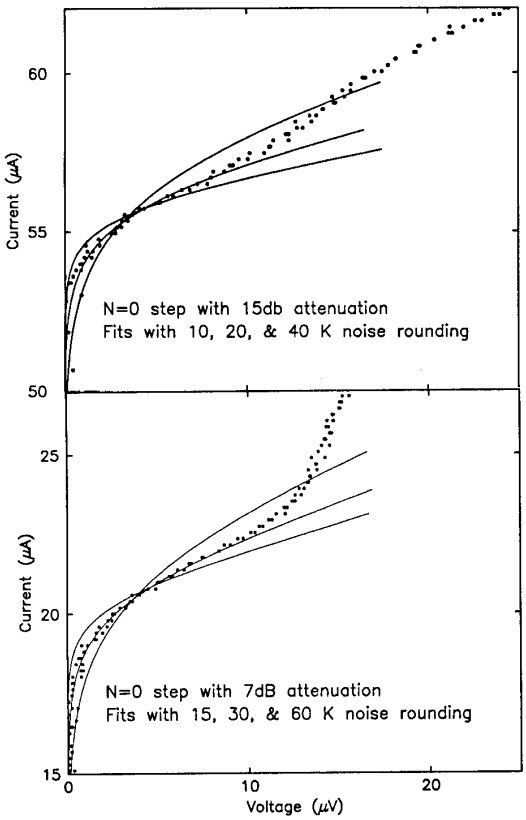


Figure 9: I-V curves exhibiting the N=0 step and N=1 step, with fits to the N=0 step assuming different noise temperatures.

radiation is also obtained at 77 K and above. But in general such weak links have sufficient self-shielding that a detailed comparison to the rf driven RSJ model cannot be easily made. Such weak links do show the onset of strong subharmonic steps (N/2, N/3, 2N/3, etc.) as the self shielding increases with decreasing temperature. This is consistent with the coupling of the rf field with flux flow along the weak link.

## Scaling of $I_CR_N$

One of the more puzzling aspects of these weak links, and weak links produced elsewhere, is the fact that the $I_CR$ product is much less then the expected value of the superconducting energy gap $\Delta$. When the low temperature (4.2 K) $I_CR$ products of the HATB microbridges studied here are examined, it is found that they obey a remarkable scaling law. For the HATB microbridges from films which showed only 45° grain boundaries on x-ray pole figures, the $I_CR$ products were proportional to $J_C^{1/2}$ with relatively little scatter. This is shown in Figure 10, which also shows some data from films on chemically polished substrates which exhibited a variety of film-substrate rotations. This latter data exhibits more scatter and a higher resistance for a given $J_C$, although a general increase in $I_CR$ with increasing $J_C$ is apparent here also. These data are largely taken from weak links with $T_C$ above 80 K, but they also include a number of points from weak links with $T_C$ at or below 60 K, and the $T_C$ seems to have no significant correlation with any variation seen.

To examine this effect further an experiment was undertaken in which oxygen was reversibly removed from the patterned films by low temperature anneals. Oxygen could be removed by a 10 sec. anneal at 500 C in Ar, and subsequently the oxygen could be replaced by a 1 min. anneal at 500 C in flowing $O_2$. From the shift in c-axis lattice constant it was estimated that $\delta$, from $YBa_2Cu_3O_{7-\delta}$, had been changed from 0 to 0.1 by the oxygen removal[13]. The departing oxygen is believed[14] to come predominantly from the chain sites which lie on the b-axis, thus allowing us to significantly alter the carrier density in the planes without otherwise altering the thin film microstructure. After this anneal is performed, the critical current of the weak link is reduced by a factor of 4 to 10, while the resistance increases by a factor of 2 to 3. Replacing the oxygen with an $O_2$ anneal results in $I_C$ and R returning to very near their original values.

If the I-V characteristics are taken at 4.2 K before annealing, after oxygen removal, and after replacing the oxygen, the scaling is demonstrated in a striking manner. If the three I-V curves from a single weak link are scaled appropriately, they are close to being identical. For 45° grain boundaries weak links which exhibit good RSJ-like I-V curves the variation is never more the 5%. When the I-V curve shows excess current or a non-linear onset of voltage, the scaling tends to work well near the onset of voltage, diverging at higher currents. From these experiments we find that 45° grain boundary weak links have an effective dynamic resistance proportional to $I_C^{-1/2}$.

## Discussion

These measurements are beginning to give a better understanding of grain boundaries weak links in general, and 45° grain boundary weak links in particular. The I-V characteristics of those weak links with low $J_C$ are well fit by the RSJ model, and weak links with higher $J_C$ show the effects of self shielding of the supercurrent, with flux flow and flux creep evident in the highest $J_C$ devices. The behavior of $I_C$ with field shows that these grain boundaries have $J_C$ which is nonuniform and asymmetric spatially, with local $J_C$'s possibly 2 to 6 times the measured values. This nonuniformity in $J_C$ suggests a possible nonuniformity in $T_C$, appearing as broader resistive transitions in some junctions, and making measurements of $I_C$ vs. T near $T_C$ difficult. The current-phase relation may be distinctly nonsinusoidal, causing an apparent high noise temperature in the microwave steps.

The most striking result is the scaling behavior of the 45° grain boundary weak links. This result, coupled with the low values of $I_CR$ observed in most high $T_C$ weak links, suggests that the transport of pairs across the weak link is somehow depressed. If we postulate that this transport is a second order tunneling process[15], rather than a first order process as in the conventional Josephson effect, we find an $I_CR^2$ scaling similar to that observed. Alternatively, the low values of $I_CR$ can be attributed to a large depression of $\Delta$ at the grain boundary, some low resistance shunting of the weak link, or a strong pair breaking process at the grain boundary. The systematic character of the effect suggests it is not due to some uncontrolled resistive shunting, while if it is due to a depression of $\Delta$ at the grain boundary, the scaling indicates that $\Delta$ is proportional to the normal conductance ($\sigma_n$) of the weak link. Finally, if we wish

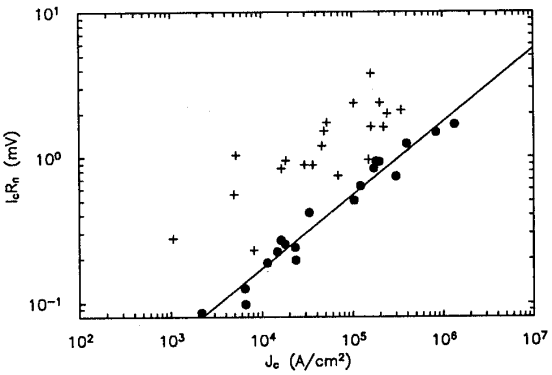


Figure 10: $I_CR_N$ (=$J_C\rho_N$) vs. $J_C$. The solid circles are data from films exhibiting only 45° tilt boundaries, with the slope of the fit being 0.505. The crosses are data from films exhibiting a range of tilt boundaries angles. In all cases the data is taken at 4.2 K.

to invoke a very strong pair breaking process as the cause of the local reduction in $\Delta$, the measured value of $\sigma_n$ compared to an ideal ballistic conductance suggests that most of the scattering at the weak link results in pair breaking.

This research was supported by the Office of Naval Research (N00014-89-J-1692) and by the Defense Advanced Research Project Agency (N00014-88-K-0374). Additional support was received from the National Science Foundation through the use of the facilities of the National Nanofabrication Facility and the Cornell Materials Science Center. We wish to specially thank Robert Yandrofski for his unique contribution to this paper.

## References

[1]S. E. Russek, D. K. Lathrop, B. H. Moeckly, R. A. Buhrman, D. H. Shin, and J. Silcox, *Appl. Phys. Lett.*, in press.

[2]J. Mannhart, P. Chaudhari, D. Dimos, C. C. Tsuei, and T. R. McGuire, *Phys. Rev. Lett.*, **61**, 2476 (1988); D. Dimos, P. Chaudhari, J. Mannhart, and F. K. LeGoues, *Phys. Rev. Lett.*, **61**, 219 (1988).

[3]B. H. Moeckly, S. E. Russek, D. K. Lathrop, R. A. Buhrman, J. Li, and J. W. Mayer, *Appl. Phys. Lett.*, in press.

[4]M. G. Norton, private communication.

[5]D. H. Shin, J. Silcox, S. E. Russek, D. K. Lathrop, B. Moeckly, and R. A. Buhrman, *Appl. Phys. Lett.*, **57**, 508 (1990).

[6]J. R. Waldram, A. B. Pippard, and J. Clarke, *Phil. Trans. Roy. Soc. Lond. A.*, **268**, 265 (1970).

[7]A. Barone and G. Paterno, "Physics and Applications of the Josephson Effect," p 191 & ch. 9, Wiley & Sons, 1982.

[8]J. Mannhart, R. Gross, K. Hipler, R. P. Huebener, C. C. Tsuei, D. Dimos, and P. Chaudhari, *Science*, **245**, 839 (1989).

[9]P. A. Lee, *J. Appl. Phys.*, **42**, 325 (1971).

[10]V. Ambegaokar and B. J. Halperin, *Phys. Rev. Lett.*, **22**, 1364 (1969).

[11]A. Barone and G. Paterno, "Physics and Applications of the Josephson Effect," ch. 4, Wiley & Sons, 1982.

[12]D. P. Hampshire, S. Chan, D. C. Larbalestier, unpublished.

[13]R. J. Cava, et. al., *Mat. Res. Soc. Symp. Proc.*, **99**, 19 (1988).

[14]F. Beech, S. Miraglia, A. Santoro, and R. S. Roth, *Phys. Rev. B*, **35**, 8788 (1987).

[15]L. G. Aslamazov, A. I. Larkin and Yu. N. Ovchinnikov, *Sov. Phys. JETP*, **28**, 171 (1969).